MOLECULAR AND CELLULAR BIOLOGY, June 2005, p. 4615–4624 Vol. 25, No. 11
0270-7306/05/$08.00+0 doi:10.1128/MCB.25.11.4615–4624.2005

Mice Deficient in Oocyte-Specific Oligoadenylate Synthetase-Like Protein OAS1D Display Reduced Fertility†

Wei Yan,[1,2] Lang Ma,[1] Paula Stein,[3] Stephanie A. Pangas,[1,4] Kathleen H. Burns,[1]‡ Yuchen Bai,[5] Richard M. Schultz,[3] and Martin M. Matzuk[1,4,6]*

Departments of Pathology,[1] Molecular and Cellular Biology,[4] and Molecular and Human Genetics,[6] Baylor College of Medicine, One Baylor Plaza, Houston, Texas 77030; Department of Physiology and Cell Biology, University of Nevada School of Medicine, Reno, Nevada 89557[2]; Department of Biology, University of Pennsylvania, Philadelphia, Pennsylvania 19104[3]; and Wyeth Research, Collegeville, Pennsylvania 19426[5]

Received 15 November 2004/Returned for modification 16 December 2004/Accepted 2 March 2005

The double-stranded RNA (dsRNA)-induced interferon response is a defense mechanism against viral infection. Upon interferon activation by dsRNA, 2′,5′-oligoadenylate synthetase 1 (OAS1A) is induced; it binds dsRNA and converts ATP into 2′,5′-linked oligomers of adenosine (called 2-5A), which activate RNase L that in turn degrades viral and cellular RNAs. In a screen to identify oocyte-specific genes, we identified a novel murine cDNA encoding an ovary-specific 2′,5′-oligoadenylate synthetase-like protein, OAS1D, which displays 59% identity with OAS1A. OAS1D is predominantly cytoplasmic and is exclusively expressed in growing oocytes and early embryos. Like OAS1A, OAS1D binds the dsRNA mimetic poly(I-C), but unlike OAS1A, it lacks 2′-5′ adenosine linking activity. OAS1D interacts with OAS1A and inhibits the enzymatic activity of OAS1A. Mutant mice lacking OAS1D (*Oas1d*$^{-/-}$) display reduced fertility due to defects in ovarian follicle development, decreased efficiency of ovulation, and eggs that are fertilized arrest at the one-cell stage. These effects are exacerbated after activation of the interferon/OAS1A/RNase L pathway by poly(I-C). We propose that OAS1D suppresses the interferon/OAS/RNase L-mediated cellular destruction by interacting with OAS1A during oogenesis and early embryonic development.

Interferons (IFN) play an important role in the host defense mechanism against viral infection (38). The 2′-5′-oligoadenylate synthetases (OASs) belong to a family of IFN-induced antiviral proteins that are highly induced by alpha/beta IFN and to a lesser extent by gamma IFN (57). OAS proteins are produced as latent enzymes, which must bind double-stranded RNA (dsRNA) to form an enzymatically active complex that catalyzes the synthesis of 2′-5′-oligoadenylates (2-5A) from ATP. The 2-5A products bind to latent endoribonuclease RNase L, leading to its dimerization, activation, and degradation of cellular and viral RNA (16, 27, 69). dsRNA produced in virus-infected cells by either viral replication or symmetric transcription of the viral genome allows OAS enzymes to sense and react to viral infection (10, 28, 44), the outcome being a global inhibition of protein synthesis that blocks viral proliferation (38).

OAS family genes have been characterized extensively in humans, and orthologous genes are also reported in mouse, rat, pig, chicken, and marine sponges (38). In humans, the OAS family consists of four classes of genes: *OAS1* (p40/p46, short form), *OAS2* (p69/p71, middle form), *OAS3* (p100, long form), and *OASL* (p59, or OAS-related protein). The three human OAS genes (OAS1 to -3) are located on chromosome segment 12q24.1 where they form a cluster within a 130-kb genomic region, representing the OAS locus (24). The gene encoding OASL has been mapped to 12q24.2 (23). The two isoforms of OAS1 (p40/p46) are identical in their first 346 amino acids but have different carboxy termini generated by alternative splicing (1). Similarly, differential splicing of the transcripts from the OAS2 gene generates the p69/p71 isoforms (33). The short form of OAS1 has one unit of the essential components for OAS enzyme activity, OAS2 has two units, and OAS3 has three catalytic units (1, 33, 40, 41). OASL has a single OAS unit and two consecutive ubiquitin-like sequences in the carboxy terminus but lacks OAS activity (21, 42). OAS1 and OAS2 are associated with different subcellular fractions, including the mitochondrial, nuclear, and rough/smooth microsomal fractions, whereas OAS3 is exclusively associated with the ribosomal fraction. Only OAS2 is myristylated, suggesting its specific interaction with membranes (34). These OAS isoforms also have different catalytic activities. OAS1 and OAS2 synthesize higher oligomeric forms of 2-5A, whereas OAS3 preferentially synthesizes 2-5A dimers (32). These differences in localization and catalytic activity among human OAS isoforms suggest that they have different functions in the 2-5A system.

Eight homologs of human *OAS1* (*Oas1a* to *-h*), two homologs of human *OSAL* (*Oasl1* and *Oasl2*), and single orthologs of human OAS2 and OAS3 have been identified in mouse (25, 46, 50). During our effort to discover oocyte-specific genes by subtractive hybridization and cDNA library screening (4, 60, 61), we identified a cDNA encoding an OAS-like protein, corresponding to the reported mouse OAS1D (26). In the present study, we report the expression, biochem-

* Corresponding author. Mailing address: Department of Pathology, Baylor College of Medicine, One Baylor Plaza, Houston, TX 77030. Phone: (713) 798-6451. Fax: (713) 798-5833. E-mail: mmatzuk@bcm.tmc.edu.

† Supplemental material for this article may be found at http://mcb.asm.org/.

‡ Present address: Department of Pathology, Johns Hopkins School of Medicine, Baltimore, MD 21287.

ical properties, and physiological roles of OAS1D during mouse oogenesis.

MATERIALS AND METHODS

Cloning of the mouse *Oas1d* cDNA and gene. We engineered a PCR suppression-subtraction ovary library (4, 60) enriched for oocyte-expressed sequences prevalent in growth differentiation factor 9 (*Gdf9*) knockout ovaries, which have a block at the primary follicle stage (12). C57BL/6J/129S6/SvEv hybrid ovaries from either *Gdf9* knockout or wild-type mice were collected and poly(A)$^+$ mRNA was made from each pool. A modified version of the PCR-Select Subtraction kit (Clontech, Palo Alto, CA) was used to generate a pBluescript SK(+) (StrataGene, La Jolla, CA) plasmid-based cDNA library. Clones from this ovarian subtractive hybridization cDNA library (pO1) were sequenced by using an Applied Biosystems 373 DNA Sequencer. BLAST searches were performed by using the NCBI databases. A partial *Oas1d* cDNA fragment (a 421-bp insert; O1-2276) identified in the above-mentioned screen was used to screen our ZAP Express (Stratagene) ovarian cDNA libraries generated from either wild-type or *Gdf9* knockout ovaries as per manufacturer's instructions and as described previously (61). In brief, approximately 300,000 clones of either wild-type or *Gdf9* knockout mouse ovary cDNA libraries were hybridized to [^{32}P]dCTP random-primed probes in Church's solution at 63°C. Filters were washed with 0.1× Church's solution and exposed overnight at −80°C. Two clones containing full-length *Oas1d* cDNA were isolated and sequenced. A similar approach was used to screen a 129S6/SvEv mouse genomic library (Stratagene), except that filters with approximately 500,000 genomic clones were hybridized. Two overlapping recombinant clones (2276-10 and 2276-4), isolated from a mouse 129S6/SvEv library, allowed us to determine the structure of the *Oas1d* genomic region and to make a targeting construct.

Northern blot analysis and in situ hybridization. Total RNA was extracted from multiple tissues of wild-type hybrid strain mice (C57BL/6J/129S6/SvEv) by using RNA STAT-60 (Leedo Medical Laboratories, Houston, TX) as described by the manufacturer. An aliquot of 12 μg of total RNA was electrophoresed on a 1.2% agarose–7.6% formaldehyde gel and transferred to Hybond-N nylon membrane (Amersham Pharmacia Biotech, Piscataway, NJ). A DNA fragment derived from the 3′UTR of the *Oas1d* cDNA was used as a probe. The membrane was hybridized, washed, and subjected to autoradiography as previously described. An 18S rRNA cDNA probe was used for the loading control. In situ hybridization of ovaries was performed as described previously (64) with the *Oas1d* cDNA fragment from the 3′-UTR. Briefly, the cDNA fragments in pGEM T-vector (Promega, Madison, WI) served as templates for generating sense and antisense strands with [^{35}S]dUTP using the Riboprobe T7/SP6 combination system (Promega). Sections were exposed to photographic emulsion (NBT-3; Kodak, Rochester, NY) for 4 to 7 days at 4°C. After the slides were developed and fixed, they were counterstained with hematoxylin. The "sense" probe revealed no hybridization (data not shown).

Generation of OAS1A and OAS1D antibodies and immunohistochemistry. The complete mouse *Oas1d* cDNA was amplified by PCR, cloned into pET-23b(+) (Novagen, Madison, WI), and sequenced to confirm the absence of mutations. Recombinant mouse OAS1A and OAS1D proteins were purified by using a Ni-NTA His-bind column according to the manufacturer's instructions (Novagen). Two goats were immunized with the purified His-tagged OAS1D or OAS1A to produce polyclonal antibodies (Cocalico Biologicals, Reamstown, PA).

Mouse ovaries were fixed in 4% paraformaldehyde in phosphate-buffered saline (PBS) overnight, embedded in paraffin, and sectioned at 5-μm thickness. Immunohistochemistry was conducted as described previously (65) with goat anti-OAS1A or OAS1D polyclonal antiserum diluted at 1:2,000. The preimmune goat serum from the same goat was used as a negative control.

Immunofluorescence. Immunofluorescence of formaldehyde-fixed unfertilized eggs and early embryos was undertaken as described previously (53, 65). Briefly, oocytes were collected and fixed in 2% formaldehyde, blocked in PBS with 10% fetal calf serum, permeabilized with Triton X-100, and treated with primary and secondary antibodies. After a washing step, DNA was counterstained with DAPI (4′,6′-diamidino-2-phenylindole), and images were obtained by using deconvolution microscopy. Both OAS1A and OAS1D antibodies were diluted 1:2,000 for immunofluorescence. All staining and imaging were performed under identical conditions within each series, and prebleed goat serum was substituted for the primary antibody to serve as a negative control.

OAS protein biochemical analyses. (i) Poly(I-C) stimulation. Twelve-week-old wild-type mice or *Oas1d*$^{-/-}$ female mice were injected intraperitoneally with 250 μg of poly(I-C) (Amersham Pharmacia Bitech., Inc., Piscataway, NJ) dissolved in physiological saline, and control mice were injected with vehicle. For Northern blot analysis, samples were collected 24 h after the injection. For superovulation experiments, pregnant mare serum gonatotropin (PMSG; 5 IU) was injected immediately after the poly(I-C) treatment.

(ii) Poly(I-C) binding assays. Poly(I-C)-agarose beads (Amersham Pharmacia) were washed three times with binding buffer A (20 mM HEPES [pH 7.5], 5 mM magnesium acetate, 10% glycerol, 0.5% NP-40, and 1 mM phenylmethylsulfonyl fluoride). An aliquot of 25 μl of beads was incubated with 10 to 20 μg of native form or fully denatured form of recombinant OAS1A or OAS1D at room temperature for 30 min on a rocking plate. The beads were then washed three times with washing buffer D (25 mM HEPES [pH 7.5], 10% glycerol, 2 mM $MgCl_2$, 0.5% NP-40, 5 mM β-mercaptoethanol, 1 mM phenylmethylsulfonyl fluoride, 1 μg of leupeptin/ml, and 1 μg of aprotinin/ml). After centrifugation, 1× sample buffer (Invitrogen) was added to the beads, followed by boiling at 100°C for 10 min. The supernatant was subjected to Western blot analysis with our goat anti-OAS1A or -OAS1D antibodies.

(iii) 2-5 OAS enzymatic activity assays. The recombinant OAS1A and OAS1D bound to poly(I-C)-agarose gel were used for 2-5 OAS activity assays as described previously (50). Briefly, the beads were suspended in 15-μl reaction buffer containing 20 mM HEPES-KOH (pH 7.5), 25 mM magnesium acetate, 50 mM KCl, 7 mM 2-mercaptoethanol, 5 mM ATP, and 20 μCi of [γ-^{32}P]ATP (NEN) and then incubated at 30°C for 4 to 12 h. The reaction mixture was heated at 95°C for 5 min, and a 2-μl portion was electrophoresed in a 20% polyacrylamide gel containing 7 M urea. Autoradiography was performed by using Kodak X-Omat AR film (Kodak, Rochester, NY).

(iv) OAS1A and OAS1D interaction assays. Mixtures of OAS1A and OAS1D (1A:1D = 2:1, 1:1, and 1: 2) or protein extracted from ovaries or oocytes were incubated in the binding buffer A at room temperature for 3 h in the presence or absence of poly(I-C) (50 μg/ml) in a 20-μl reaction volume. Next, 2 μl of goat anti-OAS1A antibody was added to the reaction, and the incubation was continued at room temperature for 1 h. The, 20 μl of protein G-Sepharose (Amersham Pharmacia Biotech, Inc., Uppsala, Sweden) was added to the mixture, followed by incubation at 4°C for 2 h. The gel was washed three times with washing buffer D and then resuspended in 1× sampling buffer (Invitrogen) for Western blot analysis with the goat anti-OAS1D antibody.

Generation of *Oas1d* knockout mice. A targeting vector for *Oas1d* was constructed containing *Pgk-HPRT* and *MC1-tk* (thymidine kinase) expression cassettes (Fig. 4A). The linearized *Oas1d* targeting vector was electroporated into AB2.2 embryonic stem (ES) cells, and ES cell clones were selected in M15 medium containing HAT (hypoxanthine, aminopterin, and thymidine) and FIAU [1-(2′-deoxy-2′-fluoro-B-D-arabinofuranosyl)-5′-iodouracil] as described previously (35). Homologous recombination was detected by Southern blot analysis with EcoRI-digested or BglII-digested DNA and 5′ or 3′ probes, respectively. Three correctly targeted ES cell clones that carried the *Oas1*^{tm1Zuk} mutation (here called *Oas1d*$^{-}$) were expanded, and these mutant ES cells were injected into C57BL/6J blastocysts to obtain chimeric mice that ultimately produced C57BL/6J/129S6/SvEv hybrid and 129 inbred F_1 heterozygous (*Oas1d*$^{+/-}$) progeny, which were intercrossed to produce *Oas1d* homozygous mutant (*Oas1d*$^{-/-}$) mice. Immunohistochemistry and Western blot analyses demonstrated no OAS1D protein in homozygous mutant ovaries (Fig. 4C and data not shown).

Oocyte collection and embryo culture. For metaphase II oocytes or in vivo-fertilized embryos, females were treated with 5 IU of PMSG, followed by 5 IU of hCG (human chorionic gonadotropin) to induce superovulation as described previously (53, 65). For fertilization, females were mated overnight with stud males, and vaginal plugs were checked the following morning. Mature metaphase II eggs and one-cell embryos were recovered from oviducts 18 to 24 h after hCG treatment in M2 medium (Sigma, St. Louis, MO) with hyaluronidase (1 mg/ml). Collections of embryos at 45, 55, and 72 h post-hCG were accomplished by flushing oviducts with M2 media. For 48-h culture experiments, eggs and embryos were kept under 5% CO_2 in M16 medium (Sigma).

TUNEL assay. Paraformaldehyde (4%)-fixed paraffin sections (5 μm) of wild-type and *Oas1d*$^{-/-}$ ovaries with or without poly(I-C) treatment were used. TUNEL (terminal deoxynucleotidyltransferase-mediated dUTP-biotin nick end labeling) assay was performed by using an ApopTag peroxidase in situ apoptosis detection kit (Intergen, Inc., Purchase, NY) according to the manufacturer's instructions.

Quantitative PCR analysis of RNA from multiple mouse tissues. Semiquantitative reverse transcription-PCR (RT-PCR) analysis was performed as reported previously (68). The primers for amplifying *Oas1a* are 5′-CTGCATCAGGA GGTGGAGTT-3′ (sense) and 5′-ACTCGGGAACCATCCTTTTT-3′ (antisense). The primers for *Oas1e* are 5′-CAGAGCAGACATCGACTCCA-3′ (sense) and 5′-CCCAAATTCCCAGACGTAGA-3′ (antisense). The primers for *Ifng* (IFN-γ) are 5′-TTTGAGGTCAACAACCCACA (sense) and 5′- CGCAA

TCACAGTCTTGGCTA-3′ (antisense). The primers for *Hprt* (loading control) are 5′-CCTGGTTAAGCAGTACAGCC-3′ (sense) and 5′-TACTAGGCAGAT GGCCACAG-3′ (antisense). To ensure the exponential amplification, the PCR cycle numbers determined experimentally were 25 cycles for *Oas1a*, 20 cycles for *Oas1e*, 20 cycles for *Ifng*, and 19 cycles for *Hprt*. All of these primer pairs encompass at least one intron to avoid amplification from genomic sequences.

Real-time PCR was performed with an ABI Prism 7500 sequence detection system with mouse *Oas1a* and *Oas1d*-specific TaqMan primer-probe sets (ABI assay ID Mm00836412_m1 and Mm00652489_m1). A total of 1 μg of total RNA from each tissue was used for RT-PCR with the TaqMan RT-PCR Universal Master mix (ABI). 18S RNA was used as an endogenous control for the normalization of each sample.

dsRNA microinjection and oocyte culture. Fully grown, germinal vesicle (GV)-intact oocytes were obtained from PMSG-primed female mice and free of attached cumulus cells as previously described (49). The collection medium was bicarbonate-free minimal essential medium (Earle's salt) supplemented with 3 mg of polyvinylpyrrolidone (PVP)/ml and 25 mM HEPES (pH 7.3) (MEM/PVP). Germinal vesicle breakdown was inhibited by including 2.5 μM milrinone (Sigma). The oocytes were transferred into CZB medium (9) containing 2.5 μM milrinone (CZB+M) and cultured in an atmosphere of 5% CO_2 in air at 37°C. Oocytes were microinjected in Whitten's medium containing 5 mM $NaHCO_3$, 15 mM HEPES (pH 7.3), 0.01% polyvinylalcohol, and 2.5 μM milrinone with 5 pl of 0.2 mg of *Mos* dsRNA/ml; the injections were performed as previously described (30). Microinjected oocytes were cultured in CZB+M for 48 h; after this time, oocytes were either radiolabeled, or they were matured in vitro for 16 h in CZB, followed by radiolabeling.

[^{35}S]methionine radiolabeling of mouse oocytes and eggs and protein electrophoresis. GV-intact oocytes or metaphase II eggs were washed through 5 drops of glutamine-free CZB and radiolabeled in this medium for 2 h with 1 mCi of [^{35}S]methionine (1,500 Ci/mmol; Amersham Biosciences, Piscataway, NJ)/ml. After being washed in MEM/PVP, groups of three to five oocytes or eggs were transferred to a microcentrifuge tube containing 40 μl of 3 mg of bovine serum albumin/ml. Trichloroacetic acid precipitation was performed as previously described (39) to determine the relative rate of protein synthesis, which was calculated as the number of acid-insoluble cpm/(number of acid-insoluble cpm + number of acid-soluble cpm) (i.e., the percent incorporation). In some experiments, groups of oocytes were transferred to a microcentrifuge tube containing 20 μl of double-strength sodium dodecyl sulfate-polyacrylamide gel electrophoresis (SDS-PAGE) sample buffer (31) and boiled for 3 min. After SDS-PAGE, the 10% gels were fixed in 10% acetic acid–30% methanol, dried, and exposed to a phosphorimager screen for 16 to 24 h. Scanning and quantification of the gel were performed by using a Storm 860 Phosphorimager and ImageQuant software (Molecular Dynamics, Inc., Sunnyvale, CA).

MAP kinase assays. Mitogen-activated protein (MAP) kinase activity was measured as previously described (55).

RESULTS

OAS1D is an oocyte-specific 2′-5′-OAS-like protein. Full-length *Oas1d* cDNA (1,730 bp) encodes a 361-amino-acid protein with 59% identity to mouse 2′,5′-oligoadenylate synthetase (OAS1A) and 72% identity with the OAS-like protein OAS1C. By Northern blot (Fig. 1A) and real-time quantitative RT-PCR (Fig. 1B) analyses, *Oas1d* mRNA was detected exclusively in the ovary, whereas *Oas1a* was ubiquitously expressed with higher levels in stomach and intestine (Fig. 1B). Since *Gdf9*$^{-/-}$ oocyte development is arrested at the primary follicle stage (13, 14, 63), the *Gdf9*$^{-/-}$ ovary proportionally contains more oocytes compared to the wild-type ovary. A significant increase in *Oas1d* mRNA levels in the *Gdf9*$^{-/-}$ ovary as determined by Northern blot analysis (Fig. 1A) strongly suggests that *Oas1d* is expressed in oocytes. As expected, our in situ hybridization study demonstrated that *Oas1d* was expressed specifically in growing oocytes at all stages of folliculogenesis (Fig. 1C).

Polyclonal goat antibodies were developed against recombinant OAS1D and reacted with a 42-kDa band exclusively in the ovary, corresponding to the predicted molecular mass of

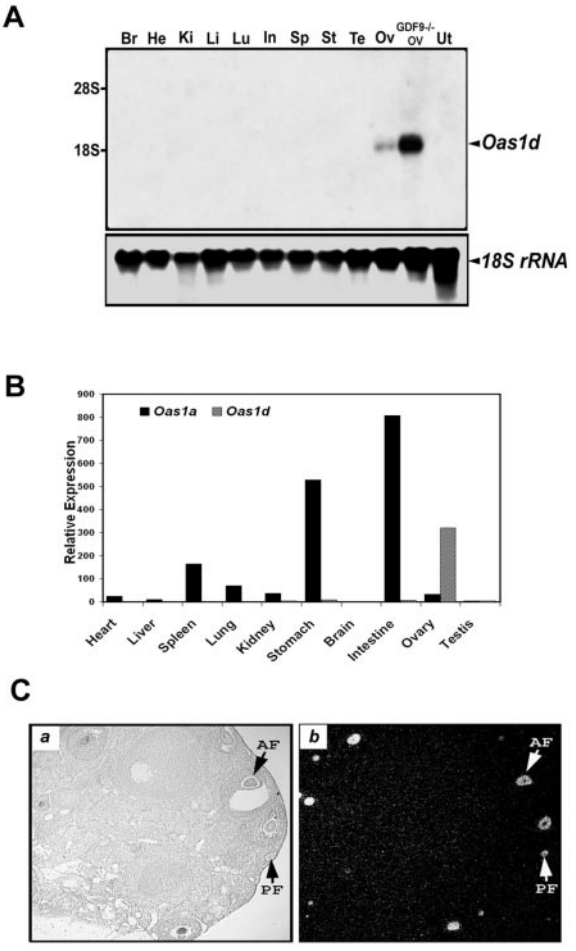

FIG. 1. *Oas1d* mRNA is exclusively expressed in growing oocytes in the ovary. (A) Northern blot analysis of *Oas1d* mRNA expression in multiple mouse tissues, including brain (Br), heart (He), kidney (Ki), liver (Li), lung (Lu), intestine (In), spleen (Sp), stomach (St), testis (Te), Ovary (Ov), *Gdf9*$^{-/-}$ ovary (GDF9$^{-/-}$ Ov), and uterus (Ut). The membrane was stripped and reprobed with an 18S rRNA cDNA probe as a loading control. (B) Real-time quantitative RT-PCR analysis of *Oas1d* and *Oas1a* mRNA expression in multiple mouse tissues. (C) In situ hybridization analysis of mouse ovarian sections. Bright (left panel) and dark (right panel) field images are shown (magnification, ×60). AF, antral follicle; PF, primary follicle.

OAS1D (Fig. 2A, top). The polyclonal goat anti-OAS1A antibodies that we prepared recognized a 46-kD band (consistent with the molecular mass of OAS1A) in multiple tissues with higher levels in the digestive tract (Fig. 2A, bottom). The antibodies appear to react specifically with their antigens because no extra bands were detected in the Western blot analyses (Fig. 2A). By immunohistochemistry, OAS1D immunoreactivity was detected in the cytoplasm of oocytes in all follicles in the adult ovary (Fig. 2B). In contrast, OAS1A immunoreactivity was present weakly not only in oocytes but also in somatic cells (Fig. 2B). Preimmune sera were used as negative controls and gave no staining (Fig. 2B).

Because OAS1D is expressed in oocytes in preovulatory follicles, we further examined its expression in isolated oocytes, zygotes, and early embryos by immunofluorescent deconvolution microscopy (Fig. 2C). OAS1A levels were relatively con-

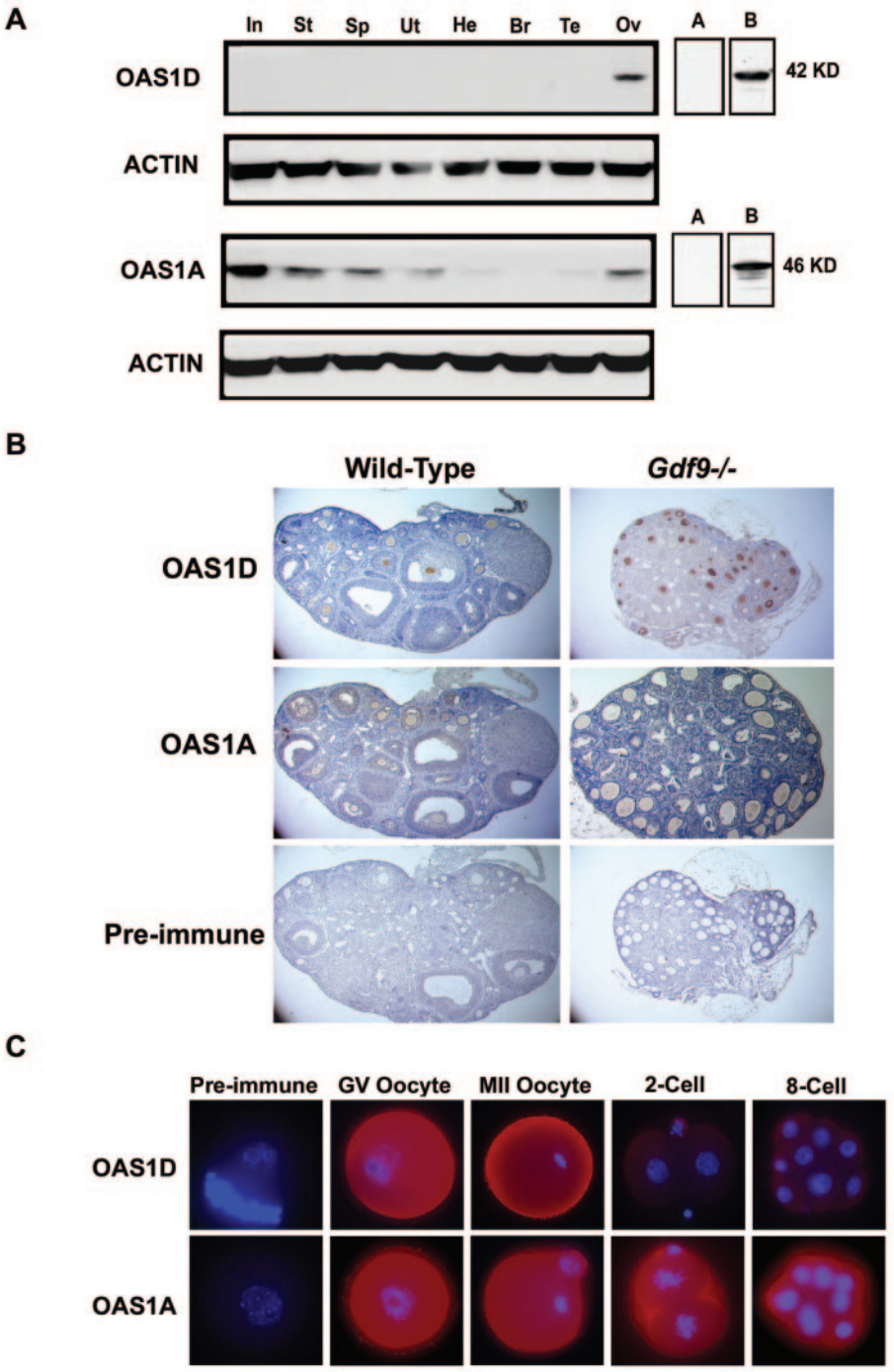

FIG. 2. OAS1D is a cytoplasmic protein exclusively expressed in oocytes and early embryos. (A) OAS1D is detected exclusively in the ovary, whereas OAS1A is ubiquitously expressed. Preimmune serum does not react with recombinant OAS1D (lane A in the upper panel), and anti-OAS1D serum does (lane B in the upper panel). Anti-OAS1A serum detects the 46 kD recombinant OAS1A band (lane A in the lower panel) and preimmune serum does not (lane B in the lower panel). (B) Immunohistochemical localization of OAS1D and OAS1A in the mouse ovary. OAS1D immunoreactivity is detected exclusively in the cytoplasm of oocytes in the wild-type or *Gdf9*$^{-/-}$ ovary, whereas OAS1A immunoreactivity is detected not only in oocytes but also in granulosa cells. Preimmune sera did not detect immunoreactive material. (C) Immunofluorescence analysis of OAS1D and OAS1A in oocytes and early embryos. OAS1D and OAS1A are stained red; DNA is stained blue with DAPI. Expression in oocytes (GV stage and metaphase II), two-cell embryos, and eight-cell embryos was analyzed on the same slide. OAS1A displays constant expression in the cytoplasm of oocytes through eight-cell embryos, whereas OAS1D levels drastically decrease after mitotic division.

stant in oocytes (GV stage and metaphase II) and in two- to eight-cell embryos (Fig. 2C). Unlike OAS1A, the levels of OAS1D diminished quickly, and OAS1D is not detected in two-cell or later embryos (Fig. 2C).

OAS1D has distinct biochemical properties compared to OAS1A. OAS1A can be induced by IFN, requires dsRNA as a cofactor, and binds and polymerizes ATP to produce 2′-5′-linked oligoadenylates (38). To analyze whether OAS1D possesses similar biochemical characteristics, we injected the dsRNA mimetic poly(I-C) intraperitoneally into adult male and female mice and, after 24 h, extracted RNA from multiple organs. Northern blot analysis was performed with specific *Oas1a* and *Oas1d* probes. In the absence of poly(I-C), *Oas1a* mRNA levels were higher in intestine and stomach but lower in other organs. However, the levels of *Oas1a* mRNA were dramatically induced in response to poly(I-C) treatment in multiple organs (Fig. 3A), which is consistent with previous studies (15, 18, 51). Whereas *Oas1a* was upregulated in response to poly(I-C) in all of the tissues examined, *Oas1d* was essentially unchanged (Fig. 3A) and remained exclusively expressed in the ovary. Like OAS1A and OAS1C (37, 50), recombinant mouse OAS1D bound the dsRNA mimetic poly(I-C) in vitro (Fig. 3B).

To determine the enzymatic activity of recombinant OAS1D in vitro, we performed 2-5A activity assays with recombinant OAS1A as a positive control. Consistent with a recent report (26), we found that OAS1D did not have 2′,5′-oligoadenylate synthetase activity (Fig. 3C). Therefore, OAS1D has biochemical properties distinct from its homolog OAS1A. OAS1D and OAS1C, together with OAS1E, OAS1G, and OAS1H (26), comprise a subfamily of the 2-5 OAS protein family, which are homologous to OAS1A, bind dsRNA, but have no 2′,5′-oligoadenylate synthetase activity. These data are consistent with a recent report suggesting that OAS1A homologs may not have enzymatic activity based on the crystal structure analysis (20).

Generation of *Oas1d*$^{-/-}$ mice. To study the functions of OAS1D in vivo, we produced *Oas1d* knockout mice. The targeting vector was designed to delete exon 1 and part of exon 2 of the *Oas1d* gene, which includes the start of transcription, the initiation ATG codon, and 157 codons of OAS1D (Fig. 4A). There is not another ATG in the coding sequences until codon 352 (3′ end of exon 5). Thus, this mutation was expected to generate a null allele.

From chimeras of three different ES cell lines, heterozygotes for the mutant *Oas1d* allele were produced. Ten male and female heterozygotes were intercrossed to produce *Oas1d* homozygous mutant male and female mice (herein called *Oas1d*$^{-/-}$). Consistent with the limited expression of *Oas1d* in embryos and adults, *Oas1d*$^{-/-}$ mice were viable and grossly normal.

Intercrossing of the F_1 heterozygotes yielded F_2 progeny, including 65 wild-type (24.4%), 134 heterozygous (50.4%), and 67 homozygous (25.2%) mice out of 31 litters analyzed. Thus, the mutant allele was transmitted with the expected Mendelian frequency of 1:2:1, and the male/female ratio was approximately 50:50 (Fig. 4B). Western blot analysis (Fig. 4C) and immunohistochemistry (data not shown) demonstrated a lack of OAS1D protein in *Oas1d*$^{-/-}$ mice, confirming that the mutant allele that we generated was null.

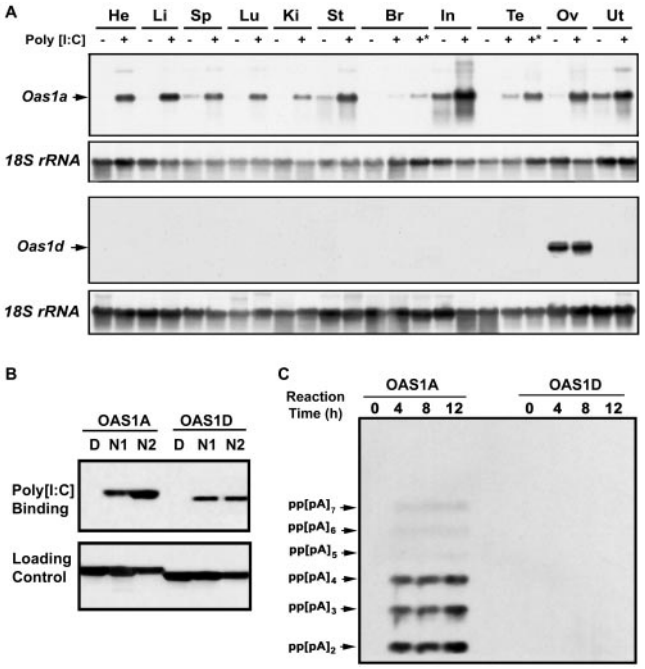

FIG. 3. Biochemical characteristics of OAS1D. (A) Poly(I-C) induces *Oas1a* but not *Oas1d* mRNA expression. Adult female and male mice were injected intraperitoneally with (+) or without (−) 250 μg of poly(I-C). In some mice, poly(I-C) was injected intratesticularly (Te, +*) or intracranially (Brain, +*). Total RNA was isolated from tissues 24 h after treatment and analyzed by Northern blot analysis with *Oas1a*, *Oas1d*, or 18S rRNA probes. *Oas1a* is induced ubiquitously, whereas *Oas1d* is not induced and continues to be expressed only in the ovary (Ov). Tissue abbreviations are the same as in the Fig. 1 legend. (B) dsRNA binding assay. Aliquots of native (N1 and N2) or fully denatured (D) His-tagged recombinant OAS1A or OAS1D were incubated with poly(I-C)-agarose, followed by washing and Western blot analysis with anti-His antibody. The same aliquot from each reaction was subjected to SDS-PAGE before incubation with poly(I-C)-agarose and was used as a loading control. (C) 2′,5′-oligoadenylate synthetase activity assay. Poly(I-C)-agarose-bound recombinant proteins were incubated with [γ-^{32}P]ATP (20 μCi) in a reaction buffer containing 20 mM HEPES-KOH, 50 mM KCl, 25 mM magnesium acetate, 7 mM 2-mercaptoethanol, and 5 mM ATP for the indicated times in hours at 33°C. The reaction mixture was centrifuged, and the supernatants were fractionated on a 20% polyacrylamide gel containing 7 M urea. The gel was dried, followed by autoradiography.

***Oas1d*$^{-/-}$ female mice display reduced fertility.** To assess the roles of OAS1D in female fertility, heterozygous and homozygous mutant females were bred for 6 months. Homozygous *Oas1d*$^{-/-}$ males displayed normal fertility. Likewise, mating of 10 *Oas1d*$^{+/-}$ females with *Oas1d*$^{+/-}$ males over 6 months resulted in 64 litters with an average litter size of 8.5 ± 0.2 pups ($n = 64$) per litter, not statistically different from the litter sizes of wild-type mice in previous experiments (8.4 ± 0.2 pups per litter, $n = 107$ [56, 63]). These findings demonstrate that *Oas1d*$^{+/-}$ females show normal fertility. Thirteen *Oas1d*$^{-/-}$ females bred to wild-type males over the same 6-month period displayed reduced fertility, with fewer pups born (5.3 ± 0.3 pups per litter, $n = 53$) in each litter and reduced litters per month (0.8 ± 0.1 pups per litter) compared to heterozygous females (1.1 ± 0.1 pups per litter) ($P < 0.01$, $n = 10$). Thus, OAS1D appears to have a role in female fertility.

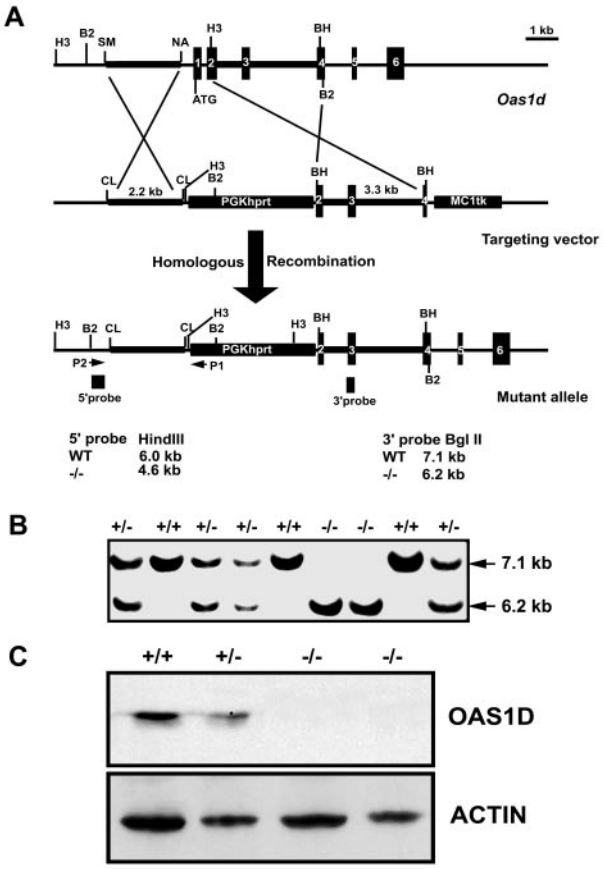

FIG. 4. Generation of *Oas1d* knockout mice. (A) *Oas1d* genomic locus and targeting vector for generation of an *Oas1d*-null allele. A deletion of exon 1 (containing the start codon) and partial exon 2 of the *Oas1d* gene was achieved by homologous recombination in AB2.2 ES cells. 5′ and 3′ probes were used to distinguish wild-type and mutant alleles. (H3, Hind III; B2, Bgl II; SM, SmaI; NA, Nar I; BH, BamH I; CL, ClaI). (B) Southern blot analysis of Bgl II-digested tail DNA from a litter of pups using the 3′ probe. The probe detects a 7.1-kb wild-type allele and a 6.2-kb mutant allele. (C) Western blot analysis of ovarian tissues from wild-type (+/+), *Oas1d* heterozygous (+/−), and *Oas1d* homozygous (−/−) mutant mice. ACTIN was detected as the loading control.

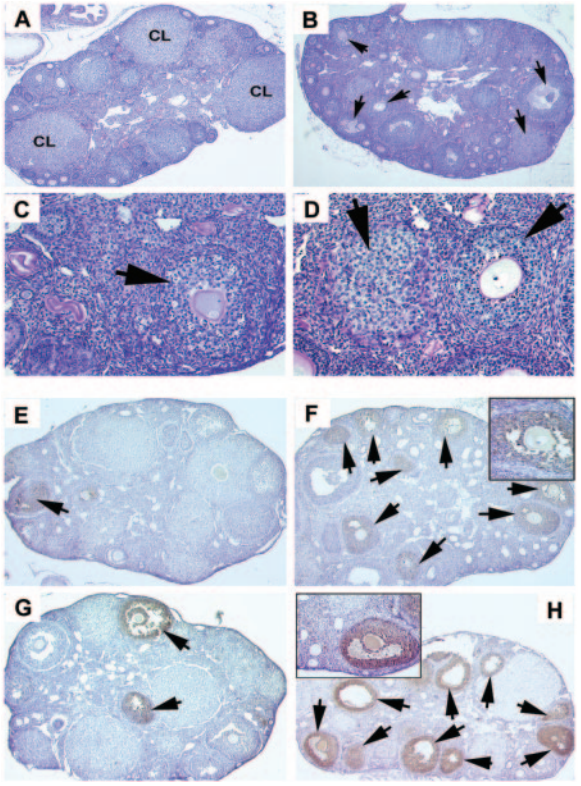

FIG. 5. Histological analyses of wild-type and *Oas1d*$^{-/-}$ ovaries. (A to D) Histology of the wild-type (A) and *Oas1d*$^{-/-}$ (B to D) ovaries. The wild-type ovary contains multiple corpus lutea (CL) and follicles at different growing stages. The *Oas1d*$^{-/-}$ ovary contains fewer CL and many degenerating follicles (arrows). High-power images (magnification, ×200) of the *Oas1d*$^{-/-}$ ovary show two areas containing several degenerating (arrows) follicles (C and D). (E to H) TUNEL assay of the wild-type (E and G) and *Oas1d*$^{-/-}$ (F and H) ovaries with (G and H) or without (E and F) poly(I-C) treatment. More TUNEL-positive follicles are present in the *Oas1d*$^{-/-}$ ovary than in the wild-type ovary with or without poly(I-C) treatment. Magnification, ×50. Insets in panels F and H show high-power images (magnification, ×400) of TUNEL-positive follicles.

To understand the cause of the reduced fertility in *Oas1d*$^{-/-}$ female mice, we first analyzed the mutant ovaries grossly and histologically. Grossly, *Oas1d*$^{-/-}$ adult ovaries were indistinguishable from those of wild-type or *Oas1d*$^{+/-}$ mice. Histological analyses of the ovaries of *Oas1d*$^{-/-}$ females at 12 wk of age revealed fewer corpora lutea compared to wild-type littermates (Fig. 5A-D). There were also more degenerating follicles in the *Oas1d*$^{-/-}$ ovaries than in wild-type ovaries. The histological observations were further confirmed by TUNEL assay, showing an increased number of TUNEL-positive follicles in the null mice (Fig. 5F) compared to wild-type mice (Fig. 5E). Moreover, a drastic increase in the number of TUNEL-positive follicles was observed in the ovaries of poly(I-C)-treated *Oas1d*$^{-/-}$ mice (Fig. 5H) compared to poly(I-C)-treated wild-type mice (Fig. 5G).

***Oas1d*$^{-/-}$ females display ovulation and preimplanation development defects.** The ovulatory functions of *Oas1d*$^{-/-}$ mice were assayed by determining the ovarian response to superovulation with exogenous gonadotropins. Wild-type and *Oas1d*$^{-/-}$ female mice were first given 5 IU of PMSG and 48 h later hCG (5 IU) and then mated with stud males. At 24 h after hCG and mating, fertilized eggs were recovered from the ampullae of the oviduct of plugged females. Fewer eggs were released by *Oas1d*$^{-/-}$ females (17.0 ± 2.3, $n = 8$) compared to wild-type (35.3 ± 4.8, $n = 8$) (Table 1). During 48-h culture in vitro, 94% of the fertilized eggs from wild-type mice developed to the eight-cell stage, whereas only 61% of the fertilized *Oas1d*$^{-/-}$ eggs progressed to the eight-cell stage (Table 1).

To analyze potential involvement of OAS1D in IFN/OAS1A-mediated cell death pathways in oocytes and early embryos, we treated wild-type and *Oas1d*$^{-/-}$ mice with poly(I-C) (250 μg) at the same time we injected PMSG (5 IU). hCG (5 IU) was given 48 h later, followed by mating with stud males. By semiquantitative RT-PCR (68), we examined the expression levels of *Ifng* (IFN-γ) and *Oas1a* in poly(I-C)-treated, nontreated, wild-type, and *Oas1d*$^{-/-}$ eight-cell embryos. Poly(I-C) treatment indeed induced IFN and OAS1A production (Fig. 6A). More interestingly, the induction of IFN

TABLE 1. Superovulation and in vivo fertilization data[a]

Genotype	No. of mice	Mean no. ± SEM of:		% Eight cell embryos
		Eggs	Eight-cell embryos	
WT	8	35.3 ± 4.8	33.2 ± 2.9	94
−/−	8	17.0 ± 2.3	10.5 ± 1.5	61
WT + poly(I-C)	6	17.2 ± 3.5*	16.2 ± 1.9*	92
−/− + poly(I-C)	6	9.6 ± 1.6*	3.2 ± 0.7*	34

[a] WT, wild type; −/−, Oas1d$^{-/-}$. Data are a summary of two independent experiments. *, $P < 0.01$.

and OAS1A appeared to be stronger in *Oas1d*$^{-/-}$ embryos than in wild-type embryos (Fig. 6A). The numbers of ovulated eggs were reduced in the poly(I-C)-treated WT females (17.2 ± 3.5, $n = 6$) compared to untreated wild-type females (35.3 ± 4.8, $n = 8$), indicating that activation of the IFN/OAS1A/RNase L pathway has an adverse effect on ovulation. The number of eggs recovered from poly(I-C)-treated *Oas1d*$^{-/-}$ female mice (9.6 ± 1.6, $n = 6$) was statistically smaller than poly(I-C)-treated wild-type females (17.2 ± 3.5, $n = 6$; $P < 0.01$). This decrease suggests that activation of the IFN/OAS1A/RNase L pathway may have more disruptive effects on ovulation in the absence of OAS1D. Alternatively, it may reflect disrupted oocyte development in *Oas1d*$^{-/-}$ mice because they start with fewer oocytes and thus may ovulate fewer eggs. However, when we cultured these eggs in vitro, 92% of fertilized eggs from poly(I-C)-treated wild-type females developed normally to the eight-cell stage after 48 h in vitro culture, whereas the majority of the fertilized eggs from poly(I-C)-treated *Oas1d*$^{-/-}$ female mice were arrested at the one-cell zygote stage and eventually fragmented (Table 1), suggesting that activation of the IFN/OAS1A/RNase L pathway may exert more adverse effects on ovulation, possibly due to the higher IFN-γ levels.

OAS1D interacts with OAS1A in vitro and in vivo. The more adverse effects of the poly(I-C) treatment on *Oas1d*$^{-/-}$ mice than on wild-type mice strongly suggest that OAS1D is involved in the IFN/OAS1A/RNase L-mediated pathway. Because OAS1D and OAS1A are both expressed in oocytes, OAS1D may directly interact with OAS1A and thus regulate OAS1A activity. To test this hypothesis, we incubated recombinant OAS1A and OAS1D at different molar ratios (OAS1A/OAS1D at 2:1, 1;1, or 1:2). After immunoprecipitation with an OAS1A antibody, Western blot analysis was performed with an OAS1D antibody (Fig. 6B). These in vitro binding assays showed that OAS1A and OAS1D could interact directly. To further confirm this finding, we isolated oocytes from superovulated wild-type female mice that had or had not been injected with poly(I-C) and then performed coimmunoprecipitation assays (Fig. 6C). Without poly(I-C) treatment, we detected OAS1D in the OAS1A immunoprecipitates from total ovary lysates (Fig. 6C, lane 1) but barely detected OAS1D from the oocyte lysate (232 to 245 oocytes) (Fig. 6C, lane 2). From poly(I-C)-treated wild-type ovary (Fig. 6C, lane 7) or oocytes (Fig. 6C, lane 4), we readily detected OAS1D in the OAS1A immunoprecipitates. These results suggest that OAS1A and OAS1D can bind each other.

OAS1D inhibits OAS1A enzymatic activity. The direct interaction between OAS1D and OAS1A is intriguing because it implied that OAS1D is involved in regulating the enzymatic

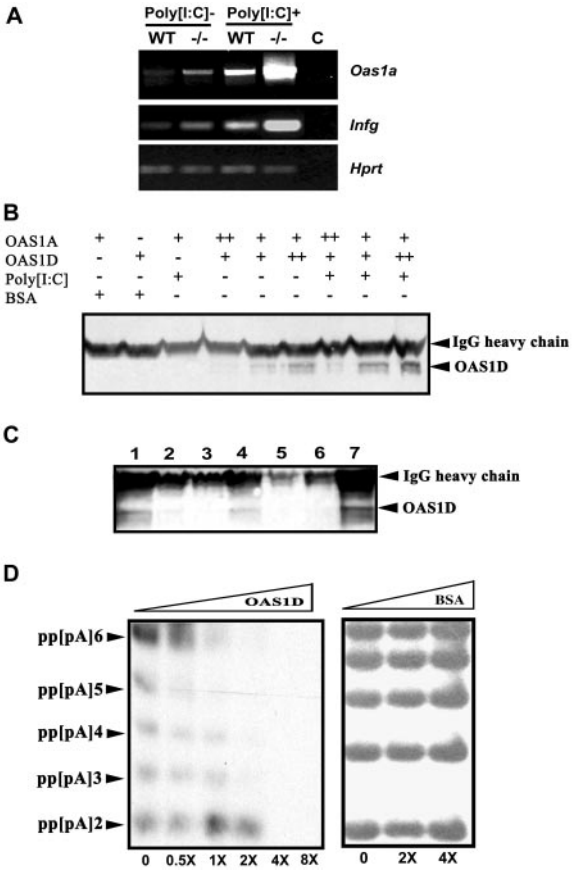

FIG. 6. Induction of IFN-γ by poly(I-C), interaction of OAS1D with OAS1A, and inhibition of OAS1A enzymatic activity by OAS1D. (A) Induction of *Ifng* (IFN-γ) and *Oas1a* by poly(I-C) treatment in eight-cell embryos. The PCR conditions are described in Materials and Methods. (B) OAS1D binds OAS1A in vitro. Recombinant OAS1A and OAS1D were incubated in a binding buffer, followed by immunoprecipitation with OAS1A antibody. The precipitates were washed and subjected to Western blot analysis with OAS1D antibody. (C) Total protein lysates from ovary (50 μg) or oocytes (232 to 245 oocytes) were immunoprecipitated with OAS1A antibody, followed by Western blot analysis with OAS1D antibody. Lanes: 1, wild-type ovary without poly(I-C) treatment; 2, wild-type oocytes without poly(I-C) treatment; 3, *Oas1d*$^{-/-}$ ovary without poly(I-C) treatment; 4, wild-type oocytes after poly(I-C) treatment; 5, *Oas1d*$^{-/-}$ ovary after poly(I-C) treatment; 6, wild-type ovary immunoprecipitated with OAS1A preimmune serum; 7, wild-type ovary after poly(I-C) treatment. (D) Inhibition of OAS1A activity by OAS1D. Six reactions containing a fixed amount of OAS1A and increasing amounts of OAS1D (0, 0.5×, 1×, 2×, 4×, or 8×) were analyzed, and OAS1D was found to completely abolish OAS1A enzymatic activity when presented in excessive amount (2× to 4×). As a specificity control, when OAS1D was replaced with excessive amounts (2× and 4×) of bovine serum albumin (BSA), no effect on the OAS1A activity was observed.

activity of OAS1A. To test this hypothesis, we measured OAS1A activity in the absence or presence of OAS1D (Fig. 6D). Interestingly, incorporating OAS1D in the 2′-5′-oligoadenylate synthesis reaction caused a dose-dependent inhibition of OAS1A activity. This indicates that OAS1D has inhibitory effects on OAS1A enzymatic activity, probably by directly binding to OAS1A and/or competing with OAS1A.

Effect of long dsRNA on protein synthesis in OAS1D-null oocytes. Mouse oocytes and preimplantation embryos, as well

as ES and embryonic carcinoma cells, apparently lack a classical IFN response to dsRNA (2, 36, 52, 54, 59, 67) that would ultimately result in a global inhibition of protein synthesis and ensuing apoptosis. In the oocyte, the PKR-mediated portion of the response may be lacking because oocytes express very low levels of PKR and its immediate target eIF2α (unpublished observations). What is puzzling is the lack of RNase L-mediated mRNA degradation. The ability of OAS1D to function as a dominant-negative protein suggests that Oas1d$^{-/-}$ oocytes can mount an IFN response, which could contribute to the observed phenotype. Accordingly, we examined the effect of microinjected long dsRNA on protein synthesis in mouse oocytes.

Both wild-type and *Oas1d*$^{-/-}$ oocytes were injected with *Mos* dsRNA and after 48 h of culture under conditions that inhibit maturation the oocytes were assayed for the relative rate of protein synthesis. The results of these experiments revealed no significant differences between any of the groups; the percentages of [^{35}S]methionine incorporation were 47.2% ± 0.9% and 45.0% ± 0.3% and 48.6% ± 1.3% and 44.6% ± 0.5% (mean ± the SEM, $n = 3$), for nontransgenic uninjected and injected oocytes and transgenic uninjected and injected oocytes, respectively; no significant differences were observed after 24 h of culture after microinjection of *Mos* dsRNA (see Fig. S1 in the supplemental material). In addition, when equal numbers of these metabolically radiolabeled oocytes were directly applied to and run on a SDS–10% PAGE gel, there were no apparent changes in the qualitative pattern of protein synthesis and the total lane intensity was the same for each sample (see Fig. S1 in the supplemental material). The *Mos* dsRNA was effective in promoting an RNAi response because when these injected OAS1D wild-type and null oocytes were matured, the maturation-associated increase in MAP kinase activity, which is a consequence of recruitment of *Mos* mRNA (55), did not occur (see Fig. S2 in the supplemental material). Moreover, these oocytes matured to metaphase II and underwent spontaneous parthenogenetic activation, which is the *Mos*-null phenotype (11, 22). The results of these experiments strongly suggest that *Oas1d*$^{-/-}$ oocytes do not mount a strong interferon response to long dsRNA.

DISCUSSION

The IFN/OAS/RNase L pathway represents a major host defense mechanism against viral infection. This pathway is also involved in regulating cell division (29), differentiation (47), and apoptosis by direct interaction with BCL2 family proteins or by regulating cellular mRNA stability and thus affecting protein biosynthesis (7, 8, 19, 70). Several tumors have a defective IFN/OAS/RNase L pathway, suggesting that dysregulation of this pathway leads to tumorigenesis (5, 6, 43, 45, 58).

In humans, three classes of OAS genes (*OAS1*, *OAS2*, and *OAS3*) and one *OAS*-like gene (*OASL*) have been reported (23, 24). In mice, there are eight *Oas1* subtype genes (*Oas1a*, *Oas1b*, *Oas1c*, *Oas1d*, *Oas1e*, *Oas1f*, *Oas1g*, and *Oas1h*) that are homologous to human *OAS1*. One OAS2 homologous gene (*Oas2*), one OAS3 homologous gene (*Oas3*), and two OASL homologous genes (*Oas11* and *Oas12*) have also been identified in the mouse (26). Among the eight OAS1 homologs, OAS1A is the only one that has 2′,5′-OAS enzymatic activity. *Oas1a* is ubiquitously expressed in multiple tissues with higher levels in digestive and lymphoid organs (46, 50). We have analyzed the expression of five *Oas1* subtypes and *Oas2* and *Oas3* genes in nine mouse tissues by semiquantitative RT-PCR (see Fig. S3 in the supplemental material) and found that *Oas1d* is the only one that displays an ovary-specific expression pattern. The ovary-specific expression of *Oas1d* prompted us to explore its physiological role during oogenesis and/or early embryogenesis by generating mutant mice lacking OAS1D.

OAS1A synthesizes oligomers of adenosine (2-5A) in response to dsRNA. Structure-function studies have shown that the P-Loop, D-Box, and KR-Rich regions of OAS1 proteins are required for catalytic activity (48, 62). The P-Loop binds dsRNA, the D-Box binds Mg^{2+}, and the KR-rich domain binds ATP for conversion to 2′,5′-oligoadenylates. In particular, mutations of K^{67}, D^{76}, D^{78}, and K^{200} in OAS1A abolish OAS enzymatic activity (48, 62). Similar to OAS1C (50) and OAS1E (26), OAS1D does not have 2′,5′-oligoadenylate synthetase activity. Comparison of mouse OAS1C-E and human OASL demonstrate that the four residues mentioned are not conserved (see Fig. S5 in the supplemental material). This is the likely reason for the absence of OAS activity in mouse OAS1C, OAS1D, and human OASL.

Because the OAS/RNase L pathway regulates viral and cellular mRNA degradation, the existence of an oocyte-specific OAS1-like protein suggests that OAS1D has a role in OAS/RNase L-mediated cellular mRNA degradation during oogenesis and/or early embryogenesis. OAS1D appears to directly interact with OAS1A and inhibit OAS1A activity. Therefore, we hypothesized that OAS1D serves as a protective factor for oocytes because it can inhibit OAS1A activity and thus block the IFN/OAS/RNase L-mediated RNA degradation pathway. Thus, the reproductive defects in *Oas1d*-null mutants would reflect the loss of OAS1D protective effects and the null oocytes become more susceptible to dsRNA-induced IFN response and cell death. Consistent with this, we see significantly decreased numbers of ovulated eggs and drastically increased fragmentation of early embryos from *Oas1d*-null mice.

Oas1d$^{-/-}$ females produce fewer eggs, and fertilized *Oas1d*-null eggs eventually arrest at the one-cell to two-cell stage transition. If OAS1D is protective in oocytes, the loss of OAS1D would result in the predisposition of *Oas1d*-null eggs to inappropriate mRNA degradation and arrest of cell growth upon dsRNA stimulation. If this hypothesis is true, then injection of long dsRNA should trigger the IFN response, which would ultimately cause degradation of mRNA leading to decreased protein synthesis. However, when *Mos* dsRNA is injected into *Oas1d*$^{-/-}$ and wild-type oocytes, no significant difference in protein synthesis is observed. It is possible that other OAS1 subtype proteins may be redundant with OASID so that *Oas1d*$^{-/-}$ oocytes still display resistance to dsRNA-triggered IFN response. Based on our semiquantitative RT-PCR analyses, *Oas1c* and *Oas1e* are also abundantly expressed in oocytes (see Fig. S3 in the supplemental material) and may compensate for the loss of OAS1D. These three OAS1A-like proteins are not only responsive to poly(I-C) stimulation but also lack enzymatic activity (Fig. S5 in the supplemental material and reference 26). However, *Oas1d*$^{-/-}$ females still display subfertility, indicating that OAS1D has unique roles that can only be partially compensated for by OAS1C and OAS1E. Generation

of knockout mice lacking OAS1C, OAS1E, or a combination of all three proteins may reveal more effects of these OAS-like proteins on female fertility.

Similar to oocytes, pluripotent embryonic cells, including embryonic carcinoma, ES, and embryonic germ cells also lack IFN inducibility and IFN sensitivity (3, 17, 66). We examined the mRNA levels of *Oas1a*, *Oas1d*, and *Oas1e* in three different ES cell lines (AB2.2, R1, and AB-1), and our results showed that whereas *Oas1d* was not expressed in these ES cells, *Oas1e*, another nonenzymatic OAS1D homolog, was abundantly expressed in these cells (Fig. S4 in the supplemental material). These data strongly imply that the presence of nonenzymatic OAS1D homologs may be responsible for the lack of IFN response in these embryonic cells and that each is functionally redundant. Thus, it may be possible to manipulate the IFN response by deletion or overexpression of these nonenzymatic homologs.

An inhibitory effect of OAS1D on the OAS1A-mediated IFN response seems to contradict a protective role of this pathway against viral infection. However, the OAS1A-mediated IFN response is ubiquitously activated upon viral infection or dsRNA stimulation and, therefore, multiple organs are implicated, as evidenced by the dramatic induction of OAS1A after dsRNA stimulation (Fig. 3A). Oogenesis is a lengthy process, and adverse effects on the mRNA degradation pathway may compromise fertility and/or early embryonic development. Abundant OAS1D, as well as OAS1C and OAS1E, in oocytes that can block the OAS1A-mediated IFN pathway may represent a protective mechanism during evolution to prevent massive loss of oocytes during an acute viral infection, therefore maintaining female fertility and continued propagation of the species. Alternatively, the OAS1A-mediated IFN response may have roles independent of viral infection, such as RNA interference, translational repression, or maintenance of mRNA stability; in these cases, OAS1D may be a critical regulator of OAS1A during these other processes.

In summary, our data reveal for the first time that OAS1D plays a role in the control of female fertility in mice. OAS1D and other nonenzymatic OAS1 subtype proteins constitute a group of proteins that may suppress the IFN/OAS/RNase L-mediated mRNA degradation, thus protecting oocytes and early embryos from cell death. The protective effects of these inactive OAS may explain the lack of an IFN response to dsRNA in oocytes. An interesting possibility is that overexpression of OAS1D may help to suppress the IFN response and may facilitate the application of dsRNA in somatic cell lineages.

ACKNOWLEDGMENTS

We thank Gregory Kopf and Emily Shen (Wyeth Research) for critical reading of the manuscript.

These studies were supported in part by National Institute of Health grants HD42500 to M.M.M. and HD22681 to R.M.S. and a research grant from Wyeth Research. W.Y. was supported by a postdoctoral fellowship from the Ernst Schering Research Foundation. S.A.P. was supported in part by a postdoctoral fellowship from Baylor's Center for Reproductive Biology (HD007165) and a National Research Service Award (F32 HD046335-01A1). K.H.B. was a student in the Medical Scientist Training Program at Baylor College of Medicine, supported in part by NIH training grant GM07330.

REFERENCES

1. **Benech, P., Y. Mory, M. Revel, and J. Chebath.** 1985. Structure of two forms of the interferon-induced (2′-5′) oligonucleotide A synthetase of human cells based on cDNAs and gene sequences. EMBO J. **4:**2249–2256.
2. **Billy, E., V. Brondani, H. Zhang, U. Muller, and W. Filipowicz.** 2001. Specific interference with gene expression induced by long, double-stranded RNA in mouse embryonal teratocarcinoma cell lines. Proc. Natl. Acad. Sci. USA **98:**14428–14433.
3. **Burke, D. C., C. F. Graham, and J. M. Lehman.** 1978. Appearance of interferon inducibility and sensitivity during differentiation of murine teratocarcinoma cells in vitro. Cell **13:**243–248.
4. **Burns, K. H., M. M. Viveiros, Y. Ren, P. Wang, F. J. DeMayo, D. E. Frail, J. J. Eppig, and M. M. Matzuk.** 2003. Roles of NPM2 in chromatin and nucleolar organization in oocytes and embryos. Science **300:**633–636.
5. **Carpten, J., N. Nupponen, S. Isaacs, R. Sood, C. Robbins, J. Xu, M. Faruque, T. Moses, C. Ewing, E. Gillanders, P. Hu, P. Bujnovszky, I. Makalowska, A. Baffoe-Bonnie, D. Faith, J. Smith, D. Stephan, K. Wiley, M. Brownstein, D. Gildea, B. Kelly, R. Jenkins, G. Hostetter, M. Matikainen, J. Schleutker, K. Klinger, T. Connors, Y. Xiang, Z. Wang, A. De Marzo, N. Papadopoulos, O. P. Kallioniemi, R. Burk, D. Meyers, H. Gronberg, P. Meltzer, R. Silverman, J. Bailey-Wilson, P. Walsh, W. Isaacs, and J. Trent.** 2002. Germline mutations in the ribonuclease L gene in families showing linkage with HPC1. Nat. Genet. **30:**181–184.
6. **Casey, G., P. J. Neville, S. J. Plummer, Y. Xiang, L. M. Krumroy, E. A. Klein, W. J. Catalona, N. Nupponen, J. D. Carpten, J. M. Trent, R. H. Silverman, and J. S. Witte.** 2002. RNASEL Arg462Gln variant is implicated in up to 13% of prostate cancer cases. Nat. Genet. **32:**581–583.
7. **Castelli, J. C., B. A. Hassel, A. Maran, J. Paranjape, J. A. Hewitt, X. L. Li, Y. T. Hsu, R. H. Silverman, and R. J. Youle.** 1998. The role of 2′-5′ oligoadenylate-activated ribonuclease L in apoptosis. Cell Death Differ. **5:**313–320.
8. **Castelli, J. C., B. A. Hassel, K. A. Wood, X. L. Li, K. Amemiya, M. C. Dalakas, P. F. Torrence, and R. J. Youle.** 1997. A study of the interferon antiviral mechanism: apoptosis activation by the 2-5A system. J. Exp. Med. **186:**967–972.
9. **Chatot, C. L., C. A. Ziomek, B. D. Bavister, J. L. Lewis, and I. Torres.** 1989. An improved culture medium supports development of random-bred 1-cell mouse embryos in vitro. J. Reprod. Fertil. **86:**679–688.
10. **Chebath, J., P. Benech, Y. Mory, P. Federman, H. Berissi, C. Gesang, J. Forman, S. Danovitch, R. Lehrer, N. Aloni, et al.** 1985. The human (2′-5′) oligoA synthetase gene, structure of its two enzyme products and quick cell blot for clinical monitoring of its activation by interferons. Prog. Clin. Biol. Res. **202:**149–161.
11. **Colledge, W. H., M. B. Carlton, G. B. Udy, and M. J. Evans.** 1994. Disruption of c-mos causes parthenogenetic development of unfertilized mouse eggs. Nature **370:**65–68.
12. **Dong, J., D. F. Albertini, K. Nishimori, T. R. Kumar, N. Lu, and M. M. Matzuk.** 1996. Growth differentiation factor-9 is required during early ovarian folliculogenesis. Nature **383:**531–535.
13. **Elvin, J. A., A. T. Clark, P. Wang, N. M. Wolfman, and M. M. Matzuk.** 1999. Paracrine actions of growth differentiation factor-9 in the mammalian ovary. Mol. Endocrinol. **13:**1035–1048.
14. **Elvin, J. A., C. Yan, P. Wang, K. Nishimori, and M. M. Matzuk.** 1999. Molecular characterization of the follicle defects in the growth differentiation factor 9-deficient ovary. Mol. Endocrinol. **13:**1018–1034.
15. **Feng, Y. F., and K. Y. Yang.** 1997. In vivo induction of rabbit 2′,5′-oligoadenylate synthetase. Sheng Wu Hua Xue Yu Sheng Wu Wu Li Xue Bao **29:**235–242.
16. **Floyd-Smith, G., E. Slattery, and P. Lengyel.** 1981. Interferon action: RNA cleavage pattern of a (2′-5′)oligoadenylate-dependent endonuclease. Science **212:**1030–1032.
17. **Francis, M. K., and J. M. Lehman.** 1989. Control of beta-interferon expression in murine embryonal carcinoma F9 cells. Mol. Cell. Biol. **9:**3553–3556.
18. **Gariglio, M., E. Cinato, S. Panico, G. Cavallo, and S. Landolfo.** 1991. Activation of interferon-inducible genes in mice by poly rI:rC or alloantigens. J. Immunother. **10:**20–27.
19. **Ghosh, A., S. N. Sarkar, T. M. Rowe, and G. C. Sen.** 2001. A specific isozyme of 2′-5′ oligoadenylate synthetase is a dual function proapoptotic protein of the Bcl-2 family. J. Biol. Chem. **276:**25447–25455.
20. **Hartmann, R., J. Justesen, S. N. Sarkar, G. C. Sen, and V. C. Yee.** 2003. Crystal structure of the 2′-specific and double-stranded RNA-activated interferon-induced antiviral protein 2′-5′-oligoadenylate synthetase. Mol. Cell **12:**1173–1185.
21. **Hartmann, R., H. S. Olsen, S. Widder, R. Jorgensen, and J. Justesen.** 1998. p59OASL, a 2′-5′ oligoadenylate synthetase like protein: a novel human gene related to the 2′-5′ oligoadenylate synthetase family. Nucleic Acids Res. **26:**4121–4128.
22. **Hashimoto, N., N. Watanabe, Y. Furuta, H. Tamemoto, N. Sagata, M. Yokoyama, K. Okazaki, M. Nagayoshi, N. Takeda, and Y. Ikawa.** 1994. Parthenogenetic activation of oocytes in c-mos-deficient mice. Nature **370:**68–71.
23. **Hovnanian, A., D. Rebouillat, E. R. Levy, M. G. Mattei, and A. G. Hovanessian.** 1999. The human 2′,5′-oligoadenylate synthetase-like gene (OASL) encoding the interferon-induced 56-kDa protein maps to chromosome 12q24.2 in the proximity of the 2′,5′-OAS locus. Genomics **56:**362–363.
24. **Hovnanian, A., D. Rebouillat, M. G. Mattei, E. R. Levy, I. Marie, A. P. Monaco, and A. G. Hovanessian.** 1998. The human 2′,5′-oligoadenylate synthetase locus

is composed of three distinct genes clustered on chromosome 12q24.2 encoding the 100-, 69-, and 40-kDa forms. Genomics **52:**267–277.
25. **Justesen, J., R. Hartmann, and N. O. Kjeldgaard.** 2000. Gene structure and function of the 2′-5′-oligoadenylate synthetase family. Cell Mol. Life Sci. **57:**1593–1612.
26. **Kakuta, S., S. Shibata, and Y. Iwakura.** 2002. Genomic structure of the mouse 2′,5′-oligoadenylate synthetase gene family. J. Interferon Cytokine Res. **22:**981–993.
27. **Kerr, I. M., and R. E. Brown.** 1978. pppA2′p5′A2′p5′A: an inhibitor of protein synthesis synthesized with an enzyme fraction from interferon-treated cells. Proc. Natl. Acad. Sci. USA **75:**256–260.
28. **Kumar, R., D. Chattopadhyay, A. K. Banerjee, and G. C. Sen.** 1988. Ribonuclease activity is associated with subviral particles isolated from interferon-treated vesicular stomatitis virus-infected cells. J. Virol. **62:**641–643.
29. **Kumar, R., L. Korutla, and K. Zhang.** 1994. Cell cycle-dependent modulation of alpha-interferon-inducible gene expression and activation of signaling components in Daudi cells. J. Biol. Chem. **269:**25437–25441.
30. **Kurasawa, S., R. M. Schultz, and G. S. Kopf.** 1989. Egg-induced modifications of the zona pellucida of mouse eggs: effects of microinjected inositol 1,4,5-trisphosphate. Dev. Biol. **133:**295–304.
31. **Laemmli, U. K.** 1970. Cleavage of structural proteins during the assembly of the head of bacteriophage T4. Nature **227:**680–685.
32. **Marie, I., J. Blanco, D. Rebouillat, and A. G. Hovanessian.** 1997. 69-kDa and 100-kDa isoforms of interferon-induced (2′-5′)oligoadenylate synthetase exhibit differential catalytic parameters. Eur. J. Biochem. **248:**558–566.
33. **Marie, I., and A. G. Hovanessian.** 1992. The 69-kDa 2-5A synthetase is composed of two homologous and adjacent functional domains. J. Biol. Chem. **267:**9933–9939.
34. **Marie, I., J. Svab, N. Robert, J. Galabru, and A. G. Hovanessian.** 1990. Differential expression and distinct structure of 69- and 100-kDa forms of 2-5A synthetase in human cells treated with interferon. J. Biol. Chem. **265:** 18601–18607.
35. **Matzuk, M. M., M. J. Finegold, J. G. Su, A. J. Hsueh, and A. Bradley.** 1992. Alpha-inhibin is a tumour-suppressor gene with gonadal specificity in mice. Nature **360:**313–319.
36. **Paddison, P. J., A. A. Caudy, and G. J. Hannon.** 2002. Stable suppression of gene expression by RNAi in mammalian cells. Proc. Natl. Acad. Sci. USA **99:**1443–1448.
37. **Patel, R. C., and G. C. Sen.** 1994. Characterization of the interactions between double-stranded RNA and the double-stranded RNA binding domain of the interferon induced protein kinase. Cell Mol. Biol. Res. **40:**671–682.
38. **Player, M. R., and P. F. Torrence.** 1998. The 2-5A system: modulation of viral and cellular processes through acceleration of RNA degradation. Pharmacol. Ther. **78:**55–113.
39. **Poueymirou, W. T., and R. M. Schultz.** 1987. Differential effects of activators of cAMP-dependent protein kinase and protein kinase C on cleavage of one-cell mouse embryos and protein synthesis and phosphorylation in one- and two-cell embryos. Dev. Biol. **121:**489–498.
40. **Rebouillat, D., and A. G. Hovanessian.** 1999. The human 2′,5′-oligoadenylate synthetase family: interferon-induced proteins with unique enzymatic properties. J. Interferon Cytokine Res. **19:**295–308.
41. **Rebouillat, D., A. Hovnanian, I. Marie, and A. G. Hovanessian.** 1999. The 100-kDa 2′,5′-oligoadenylate synthetase catalyzing preferentially the synthesis of dimeric pppA2′p5′A molecules is composed of three homologous domains. J. Biol. Chem. **274:**1557–1565.
42. **Rebouillat, D., I. Marie, and A. G. Hovanessian.** 1998. Molecular cloning and characterization of two related and interferon-induced 56-kDa and 30-kDa proteins highly similar to 2′-5′ oligoadenylate synthetase. Eur. J. Biochem. **257:**319–330.
43. **Rennert, H., D. Bercovich, A. Hubert, D. Abeliovich, U. Rozovsky, A. Bar-Shira, S. Soloviov, L. Schreiber, H. Matzkin, G. Rennert, L. Kadouri, T. Peretz, Y. Yaron, and A. Orr-Urtreger.** 2002. A novel founder mutation in the RNASEL gene, 471delAAAG, is associated with prostate cancer in Ashkenazi Jews. Am. J. Hum. Genet. **71:**981–984.
44. **Rice, A. P., R. Duncan, J. W. Hershey, and I. M. Kerr.** 1985. Double-stranded RNA-dependent protein kinase and 2-5A system are both activated in interferon-treated, encephalomyocarditis virus-infected HeLa cells. J. Virol. **54:**894–898.
45. **Rokman, A., T. Ikonen, E. H. Seppala, N. Nupponen, V. Autio, N. Mononen, J. Bailey-Wilson, J. Trent, J. Carpten, M. P. Matikainen, P. A. Koivisto, T. L. Tammela, O. P. Kallioniemi, and J. Schleutker.** 2002. Germline alterations of the RNASEL gene, a candidate HPC1 gene at 1q25, in patients and families with prostate cancer. Am. J. Hum. Genet. **70:**1299–1304.
46. **Rutherford, M. N., A. Kumar, A. Nissim, J. Chebath, and B. R. Williams.** 1991. The murine 2-5A synthetase locus: three distinct transcripts from two linked genes. Nucleic Acids Res. **19:**1917–1924.
47. **Salzberg, S., T. Hyman, H. Turm, Y. Kinar, Y. Schwartz, U. Nir, F. Lejbkowicz, and E. Huberman.** 1997. Ectopic expression of 2-5A synthetase in myeloid cells induces growth arrest and facilitates the appearance of a myeloid differentiation marker. Cancer Res. **57:**2732–2740.
48. **Saraste, M., P. R. Sibbald, and A. Wittinghofer.** 1990. The P-loop–a common motif in ATP- and GTP-binding proteins. Trends Biochem. Sci. **15:**430–434.
49. **Schultz, R. M., R. R. Montgomery, P. F. Ward-Bailey, and J. J. Eppig.** 1983. Regulation of oocyte maturation in the mouse: possible roles of intercellular communication, cAMP, and testosterone. Dev. Biol. **95:**294–304.
50. **Shibata, S., S. Kakuta, K. Hamada, Y. Sokawa, and Y. Iwakura.** 2001. Cloning of a novel 2′,5′-oligoadenylate synthetase-like molecule, Oasl5 in mice. Gene **271:**261–271.
51. **Sokawa, Y.** 1980. Induction of poly(I):poly(C)-binding 50 K protein and 2′,5′-oligoadenylate synthetase in interferon-treated mouse L929 cells. J. Biochem. **88:**159–166.
52. **Stein, P., P. Svoboda, and R. M. Schultz.** 2003. Transgenic RNAi in mouse oocytes: a simple and fast approach to study gene function. Dev. Biol. **256:**187–193.
53. **Suzumori, N., K. H. Burns, W. Yan, and M. M. Matzuk.** 2003. RFPL4 interacts with oocyte proteins of the ubiquitin-proteasome degradation pathway. Proc. Natl. Acad. Sci. USA **100:**550–555.
54. **Svoboda, P., P. Stein, M. Anger, E. Bernstein, G. J. Hannon, and R. M. Schultz.** 2004. RNAi and expression of retrotransposons MuERV-L and IAP in preimplantation mouse embryos. Dev. Biol. **269:**276–285.
55. **Svoboda, P., P. Stein, H. Hayashi, and R. M. Schultz.** 2000. Selective reduction of dormant maternal mRNAs in mouse oocytes by RNA interference. Development **127:**4147–4156.
56. **Varani, S., J. A. Elvin, C. Yan, J. DeMayo, F. J. DeMayo, H. F. Horton, M. C. Byrne, and M. M. Matzuk.** 2002. Knockout of pentraxin 3, a downstream target of growth differentiation factor-9, causes female subfertility. Mol. Endocrinol. **16:**1154–1167.
57. **Wallach, D., M. Fellous, and M. Revel.** 1982. Preferential effect of gamma interferon on the synthesis of HLA antigens and their mRNAs in human cells. Nature **299:**833–836.
58. **Wang, L., S. K. McDonnell, D. A. Elkins, S. L. Slager, E. Christensen, A. F. Marks, J. M. Cunningham, B. J. Peterson, S. J. Jacobsen, J. R. Cerhan, M. L. Blute, D. J. Schaid, and S. N. Thibodeau.** 2002. Analysis of the RNASEL gene in familial and sporadic prostate cancer. Am. J. Hum. Genet. **71:**116–123.
59. **Wianny, F., and M. Zernicka-Goetz.** 2000. Specific interference with gene function by double-stranded RNA in early mouse development. Nat. Cell Biol. **2:**70–75.
60. **Wu, X., M. M. Viveiros, J. J. Eppig, Y. Bai, S. L. Fitzpatrick, and M. M. Matzuk.** 2003. Zygote arrest 1 (Zar1) is a novel maternal-effect gene critical for the oocyte-to-embryo transition. Nat. Genet. **33:**187–191.
61. **Wu, X., P. Wang, C. A. Brown, C. A. Zilinski, and M. M. Matzuk.** 2003. Zygote arrest 1 (Zar1) is an evolutionarily conserved gene expressed in vertebrate ovaries. Biol. Reprod. **69:**861–867.
62. **Yamamoto, Y., D. Sono, and Y. Sokawa.** 2000. Effects of specific mutations in active site motifs of 2′,5′-oligoadenylate synthetase on enzymatic activity. J. Interferon Cytokine Res. **20:**337–344.
63. **Yan, C., P. Wang, J. DeMayo, F. J. DeMayo, J. A. Elvin, C. Carino, S. V. Prasad, S. S. Skinner, B. S. Dunbar, J. L. Dube, A. J. Celeste, and M. M. Matzuk.** 2001. Synergistic roles of bone morphogenetic protein 15 and growth differentiation factor 9 in ovarian function. Mol. Endocrinol. **15:**854–866.
64. **Yan, W., K. H. Burns, L. Ma, and M. M. Matzuk.** 2002. Identification of Zfp393, a germ cell-specific gene encoding a novel zinc finger protein. Mech. Dev. **118:**233–239.
65. **Yan, W., A. Rajkovic, M. M. Viveiros, K. H. Burns, J. J. Eppig, and M. M. Matzuk.** 2002. Identification of Gasz, an evolutionarily conserved gene expressed exclusively in germ cells and encoding a protein with four ankyrin repeats, a sterile-alpha motif, and a basic leucine zipper. Mol. Endocrinol. **16:**1168–1184.
66. **Yang, S., S. Tutton, E. Pierce, and K. Yoon.** 2001. Specific double-stranded RNA interference in undifferentiated mouse embryonic stem cells. Mol. Cell. Biol. **21:**7807–7816.
67. **Yu, J., M. Deng, S. Medvedev, J. Yang, N. B. Hecht, and R. M. Schultz.** 2004. Transgenic RNAi-mediated reduction of MSY2 in mouse oocytes results in reduced fertility. Dev. Biol. **268:**195–206.
68. **Zheng, H., W. Yan, J. Toppari, and P. Harkonen.** 2000. Improved nonradioactive RT-PCR method for relative quantification of mRNA. BioTechniques **28:**832–834.
69. **Zhou, A., B. A. Hassel, and R. H. Silverman.** 1993. Expression cloning of 2-5A-dependent RNase: a uniquely regulated mediator of interferon action. Cell **72:**753–765.
70. **Zhou, A., J. Paranjape, T. L. Brown, H. Nie, S. Naik, B. Dong, A. Chang, B. Trapp, R. Fairchild, C. Colmenares, and R. H. Silverman.** 1997. Interferon action and apoptosis are defective in mice devoid of 2′,5′-oligoadenylate-dependent RNase L. EMBO J. **16:**6355–6363.